

Proton form-factor dependence of the finite-size correction to the Lamb shift in muonic hydrogen

J. D. Carroll* and A. W. Thomas
*Centre for the Subatomic Structure of Matter (CSSM),
 Department of Physics, University of Adelaide, SA 5005, Australia*[†]

J. Rafelski
Departments of Physics, University of Arizona, Tucson, Arizona, 85721 USA

G. A. Miller
University of Washington, Seattle, WA 98195-1560 USA
 (Dated: October 15, 2018)

The measurement of the $2P_{3/2}^{F=2}$ to $2S_{1/2}^{F=1}$ transition in muonic hydrogen by Pohl *et al.* [1] and subsequent analysis has led to the conclusion that the rms radius of the proton differs from the accepted (CODATA) [2] value by approximately 4%, corresponding to a 4.9σ discrepancy. We investigate the finite-size effects—in particular the dependence on the shape of the proton electric form-factor—relevant to this transition using bound-state QED with nonperturbative, relativistic Dirac wave-functions for a wide range of idealised charge-distributions and a parameterization of experimental data in order to comment on the extent to which the perturbation-theory analysis which leads to the above conclusion can be confirmed. We find no statistically significant dependence of this correction on the shape of the proton form-factor.

PACS numbers: 36.10.Ee, 31.30.jr, 03.65.Pm, 32.10.Fn

I. INTRODUCTION

The measurement and subsequent analysis of the $2P_{3/2}^{F=2}$ to $2S_{1/2}^{F=1}$ transition by Pohl *et al.* [1] concludes that the proton rms charge-radius is approximately 4% smaller than previously accepted (as per the 2006 CODATA¹ value [2]). If accurate, this would indicate that either QED is an incomplete description of the contributions to the transition, something has been missed, or something has been incorrectly calculated.

Following the work of Refs. [3–5], we focus on one particular contribution to this transition, namely the finite-size correction to the $2P_{1/2}$ – $2S_{1/2}$ Lamb shift. We report on the form-factor dependence of this correction as well as the implications for the analysis leading to the proton rms charge-radius. Discussions of the form-factor dependence of finite-size effects have recently been reignited by de Rújula [6] and this work should settle claims made in that reference.

II. NUMERICAL METHOD

The numerical method used here has recently been summarised in Carroll *et al.* [7] and will not be repeated here. The highly abridged description is that we use an effective Dirac equation for a muon (with a reduced

mass appropriate to the μ -p system). This is expected to provide a precise approximation to the two-particle Bethe-Salpeter equation, yielding accurate muon wave-functions for the various potentials studied.

The eigenvalues for each eigenstate can be calculated by inserting the various potentials into the effective Dirac equation and integrating iteratively to produce the converged wave-function. Accuracy is controlled by comparing the converged eigenvalues with those calculated using a virial theorem and errors are conservatively found to be $\pm 0.5 \mu\text{eV}$.

III. PROTON FINITE-SIZE CORRECTIONS

As a first non-perturbative approximation, the Lamb shift in hydrogen is calculated using the point-Coulomb and point vacuum polarization potentials

$$\begin{aligned} V(r) &= V_C + V_{\text{VP}}(r) \\ &= -\frac{Z\alpha}{r} \\ &\quad - \frac{Z\alpha}{r} \frac{\alpha}{3\pi} \int_4^\infty \frac{e^{-m_e qr}}{q^2} \sqrt{1 - \frac{4}{q^2}} \left(1 + \frac{2}{q^2}\right) d(q^2), \end{aligned} \quad (1)$$

where here m_e represents the electron mass which arises as this is a consideration of the production of a virtual electron-positron pair. The momentum integration variable has been changed to $d(q^2)$, perhaps disguising the fact that the lower cut-off of $q^2 = 4$ corresponds to $q = 2m_e$ —the energy required to produce the pair.

*Electronic address: jcarroll@physics.adelaide.edu.au

[†]URL: <http://www.physics.adelaide.edu.au/cssm>

¹ Recently updated: <http://physics.nist.gov/cgi-bin/cuu/Value?r>

These potentials can be modified to account for the finite-size of the proton by convoluting the point potential with the proton charge-distribution. For example, the modification of the Coulomb potential gives the Fourier transform of the Coulomb potential in atoms

$$\tilde{V}(\vec{q}) = -Z\alpha 4\pi \frac{G_E(\vec{q}^2)}{\vec{q}^2}, \quad (2)$$

where we note that as the energy transfer to the proton is essentially negligible, \vec{q}^2 and the invariant, Q^2 , are functionally identical. The coordinate-space potential can then be written in terms of a three-dimensional Fourier transform of $G_E(\vec{q}^2)$:

$$\rho(r) \equiv \int \frac{d^3q}{(2\pi)^3} e^{-i\vec{q}\cdot\vec{r}} G_E(\vec{q}^2), \quad (3)$$

as

$$V_C(r) = -\frac{Z\alpha}{r} \rightarrow -Z\alpha \int \frac{\rho(r')}{|\vec{r} - \vec{r}'|} d^3r'. \quad (4)$$

Since the potential of Eq. (4) involves the proton charge-distribution $\rho(r)$ —itself a function of the rms charge-radius—this leads to a radius-dependent quantity. The dependence on the choice of charge-distribution is investigated here. We enforce that a charge-distribution must satisfy

$$\int \rho(r) d^3r = 1, \quad (5)$$

and we can investigate the effect of using different forms for $\rho(r)$. If we use, say, an exponential form (corresponding to a dipole form-factor, see Eq. (21))

$$\rho(r) = Ae^{-Br}, \quad (6)$$

then we can define the rms charge-radius via a ratio of the moments of the charge-distribution, as

$$\langle r^2 \rangle = \frac{\int r^2 \rho(r) d^3r}{\int \rho(r) d^3r}, \quad (7)$$

for which the value of A in Eq. (6) is arbitrary, and which can be rearranged such that we arrive at $B = \sqrt{12/\langle r_p^2 \rangle}$ (and $A = B^3/8\pi$ in order to correctly normalise the distribution). The normalized exponential charge-distribution is then given by

$$\rho_E(r) = \frac{\eta^3}{8\pi} e^{-\eta r}; \quad \eta = \sqrt{12/\langle r_p^2 \rangle}. \quad (8)$$

We can, however, perform the same procedure for alternative charge-distributions and determine the dependence on this choice. For a Gaussian charge-distribution

—corresponding to a Gaussian form-factor—the normalised form is given by

$$\rho_G(r) = \left(\frac{\eta'}{\pi}\right)^{3/2} e^{-\eta' r^2}; \quad \eta' = 3/2\langle r_p^2 \rangle. \quad (9)$$

Similarly, for a Yukawa charge-distribution—corresponding to a monopole form-factor—the normalized form is given by

$$\rho_Y(r) = \left(\frac{\eta''}{4\pi}\right) e^{-\eta'' r/r}; \quad \eta'' = \sqrt{6/\langle r_p^2 \rangle}. \quad (10)$$

To ensure that we are considering realistic distributions, we also include in our analysis a charge distribution extracted from a fit to experimental data of the Sachs electric form factor of the proton [11] $G_E(Q^2)$ given in that reference by

$$G_E(Q^2) = \frac{1 + q_6\tau + q_{10}\tau^2 + q_{14}\tau^3}{1 + q_2\tau + q_4\tau^2 + q_8\tau^3 + q_{12}\tau^4 + q_{16}\tau^5}, \quad (11)$$

for which the values of q_i are given in Table I, and for which $\tau = Q^2/4M_P^2$. This parameterization is constrained at $\mathcal{O}(Q^2)$ by

$$\lim_{Q^2 \rightarrow 0} G_E(Q^2) = 1 - Q^2 \frac{\langle r_p^2 \rangle}{6} + \mathcal{O}(Q^4) \quad (12)$$

to reproduce $\sqrt{\langle r_p^2 \rangle} = 0.878$ fm. The charge distribution for this form factor is calculated via a Fourier transform of G_E . We will herein refer to this distribution as ‘ G_E fitted’.

We note several efforts [8, 9] to include an additional ‘Darwin-Foldy’ (or similarly named) contribution to the definition of the charge radius beyond that determined in Eq. (7) and used in Eq. (12). We note that the Darwin-Foldy term was explicitly calculated by Barker and Glover [10] as part of the Breit potential. Together with the other terms in the Breit potential this is already included in the recoil correction to the Lamb shift as calculated by previous authors (e.g. [3]) and as such appears in the complete analysis determining r_p (Line 17 of Table 1 of Ref. [1] supplementary).

The model charge-distributions used in our analysis are plotted for comparison in Fig. 1 and we note the striking differences between the shapes below $r = 0.8$ fm. These are plotted again in Fig. 2 where they are weighted by $4\pi r^2$ (as used in the normalization) and though the differences are reduced, they remain non-trivial.

We can use these charge-distributions (calculated at each of four selected rms charge-radii spanning 0.2 fm surrounding the values given in Refs. [1] and [2]) to calculate the finite-size Coulomb potential of Eq. (4) — which is plotted in Fig. 3—and hence the converged Dirac wave-functions in response to this, in order to calculate the eigen-energies λ_α of the $2S_{1/2}$ and $2P_{1/2}$ eigenstates for each charge-distribution. We can then calculate

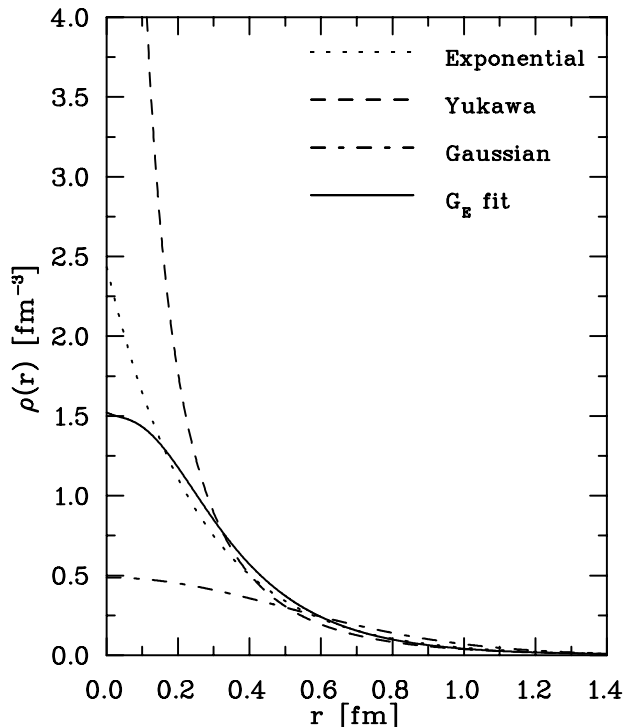


FIG. 1: Comparison of exponential, Yukawa, Gaussian, and G_E -fitted charge-distributions, each normalized to unity as per Eq. (5), calculated for $\sqrt{\langle r_p^2 \rangle} = 0.878$ fm. Note the striking differences between the shapes below $r = 0.8$ fm. The dipole distribution is nearest to the G_E -fitted distribution, as expected.

the deviation of the Lamb shifts ($\delta = \lambda_{2S} - \lambda_{2P}$) calculated in the point-Coulomb and finite-Coulomb cases to determine the magnitude of the correction

$$\Delta E_{\text{finite}} = \delta_{\text{finite}} - \delta_{\text{point}}. \quad (13)$$

We calculate the proton finite-size correction to the Lamb shift using the aforementioned effective Dirac equation method for several choices of charge-distribution

TABLE I: Coefficients of polynomial fit to Sachs electric form factor data for the proton taken from [11] as used in Eq. (12).

i	q_i
2	14.5187212
4	40.88333
6	2.90966
8	99.999998
10	-1.11542229
12	0.00004579
14	0.003866171
16	10.3580447

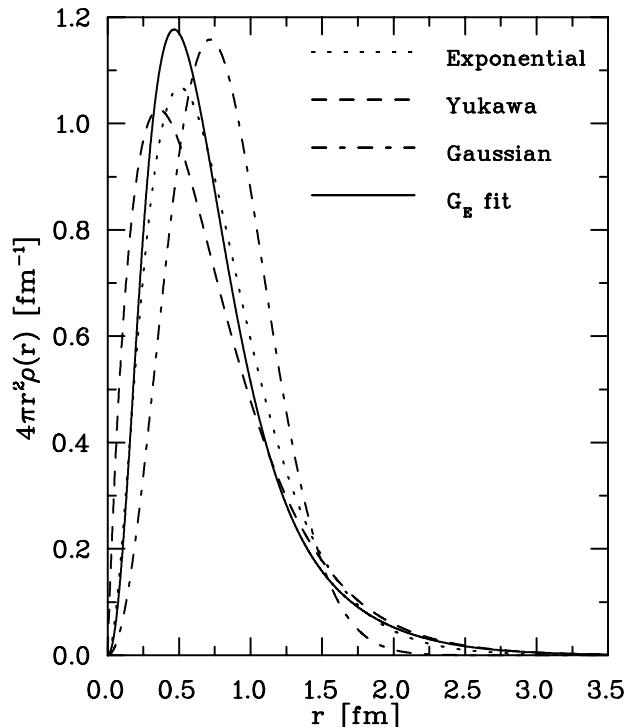


FIG. 2: Comparison of exponential, Yukawa, Gaussian, and G_E -fitted charge-distributions weighted appropriately as they contribute to the Lamb shift, each normalized to unity as per Eq. (5), calculated for $\sqrt{\langle r_p^2 \rangle} = 0.878$ fm. Here the differences are perhaps not as striking, but still noticeably different.

(viz exponential, Gaussian, and Yukawa) at several separated values of the proton rms charge-radius (viz $\sqrt{\langle r_p^2 \rangle} = 0.7$ fm, 0.84184 fm, 0.8768 fm, 0.9 fm). With this information, we calculate a polynomial fit to the data of the form

$$\Delta E_{\text{finite}} = a\langle r^2 \rangle + b\langle r^2 \rangle^{3/2}, \quad (14)$$

in order to compare with other published data. A discussion of the role of finite proton size in vacuum polarization potential is given in Ref. [7], Table I.. The relevant parameters of our fits are shown in Table II, and we find no significant dependence on the shape of the proton charge distribution.

Moreover, we are able to make a comparison to the perturbative finite-size correction (due to the finite-Coulomb potential) to the Lamb shift as referenced in Ref. [1] and derived in full in Ref. [14] as

$$\Delta E_{\text{finite}} = -\frac{2\pi}{3}Z\alpha\frac{(Z\alpha\mu)^3}{2^3\pi}\left[\langle r_p^2 \rangle - \frac{Z\alpha\mu}{2}\langle r_p^3 \rangle + (Z\alpha)^2(F_{\text{Rel}} + \mu^2 F_{\text{NR}})\right], \quad (15)$$

with the caveat that this expression was derived for an exponential charge distribution (corresponding to a dipole form-factor) and does not equally apply for other distributions. The derivation of Eq. (15) assumes that the

Schrödinger wave-function is appropriate, in that the value at the origin

$$|\phi_n(0)|^2 = \frac{(Z\alpha\mu)^3}{n^3\pi} \quad (16)$$

appears, and as such this expression requires a relativistic correction F_{Rel} . Alternatively, by numerically calculating the converged Dirac wave-functions we require no such perturbative correction, and a comparison with that given in Eq. (15) is consistent. We find agreement between our Dirac calculation with an exponential distribution and various evaluations of Eq. (15) to within 0.05%, as detailed in Table II.

As the fit to the experimental form factor data is performed at a single value of r_p we cannot determine a polynomial dependence on this quantity. We can however interpolate the shifts from our three models to compare at a single value of r_p . The result of such a comparison is that at $r_p = 0.878$ fm, the contribution to the Lamb shift due to the finite size of the proton is given by

$$\Delta E_{\text{finite}}^{\text{Exponential}}(0.878 \text{ fm}) = -3.9850 \text{ meV}, \quad (17)$$

$$\Delta E_{\text{finite}}^{\text{Yukawa}}(0.878 \text{ fm}) = -3.9830 \text{ meV}, \quad (18)$$

$$\Delta E_{\text{finite}}^{\text{Gaussian}}(0.878 \text{ fm}) = -3.9868 \text{ meV}, \quad (19)$$

$$\Delta E_{\text{finite}}^{G_E \text{ fitted}}(0.878 \text{ fm}) = -3.9799 \text{ meV}, \quad (20)$$

in keeping with our conclusion that the form-factor shape is of negligible influence.

We note Ref. [12] in which a choice of electric form-factor parameterization is compared to an idealized dipole form-factor

$$G_D(Q^2) = (1 + Q^2/\Lambda^2)^{-2}, \quad (21)$$

and for which the ratio of the two tends to unity at low Q^2 . The ratio remains close to unity up to approximately 1 (GeV/c)², re-enforcing that a dipole is a suitable parameterization of the electric form-factor for the purposes of this analysis.

IV. IMPLICATIONS FOR THE PROTON RADIUS

With the parameterizations of the finite-size contribution to the Lamb shift determined, it is possible to infer a proton rms charge radius $\langle r_p^2 \rangle^{1/2}$ by re-analyzing the measured transition in muonic hydrogen of Ref. [1]. If we take all other contributions to the transition *prima facie* (we note that because of the unknown magnitude of off-shell corrections to the photon-nucleon vertex [15] such an analysis is physically inappropriate) we can solve the cubic equation

$$L_{\text{measured}} = L_{\text{r-indep}} + a'\langle r^2 \rangle + b'\langle r^2 \rangle^{3/2}, \quad (22)$$

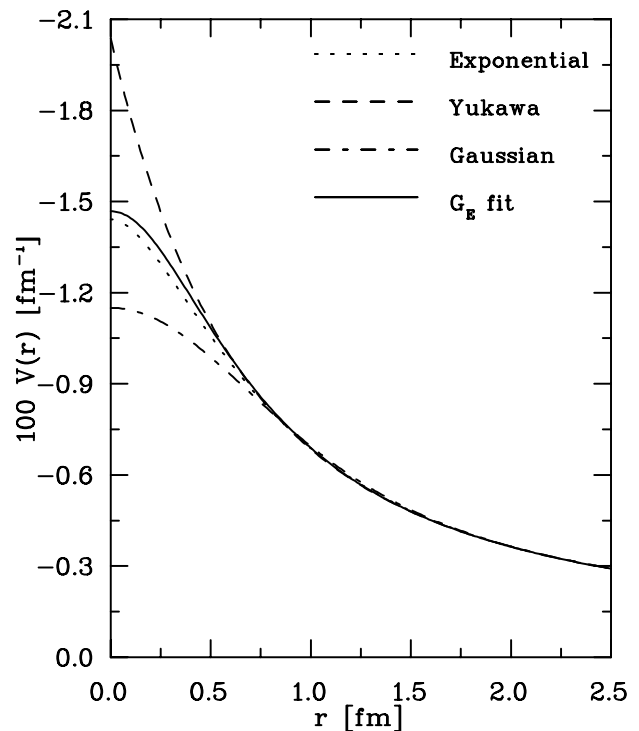


FIG. 3: Comparison of exponential, Yukawa, Gaussian, and G_E -fitted finite-size Coulomb potentials calculated for $\sqrt{\langle r_p^2 \rangle} = 0.878$ fm.

(where we note that a' and b' may also account for finite-size effects in the $2S$ hyperfine splitting [7], not included here, and thus $a' = a$, $b' = b$) in which the measured transition energy is $L_{\text{measured}} = 206.2949 \pm 0.0032$ meV; the sum of theoretical radius-independent contributions to the transition are $L_{\text{r-indep}} = 209.9779 \pm 0.0049$ meV (including the full Lamb shift and corrections found in [1]);

TABLE II: Coefficients of polynomial fits to the finite-size correction to the Lamb shift $\Delta E_{\text{finite}}^{\text{Lamb}}$ (refer to Eq. (14)) in muonic hydrogen for several choices of charge-distribution (calculated using the finite-Coulomb potential), and selected published values. All values in this table include a radiative correction of $-0.0275 \langle r_p^2 \rangle$ as per Ref. [1]. We note that the finite-size effects of the vacuum polarization alter these values further, and a discussion of this matter can be found in Ref. [7].

Name	$\rho(r)$	$a [\propto \langle r^2 \rangle]$	$b [\propto \langle r^2 \rangle^{3/2}]$
exponential	Ae^{-Br}	-5.2276	0.0351
Yukawa	Ae^{-Br}/r	-5.2275	0.0378
Gaussian	Ae^{-Br^2}	-5.2276	0.0323
Ref. [1]		-5.22495	0.0347
Ref. [3]		-5.22456	0.0346
Ref. [13]		-5.2249	0.0363

TABLE III: Proton rms charge-radius $\sqrt{\langle r_p^2 \rangle}$ calculated using various charge-distributions. In these calculations, the remaining analysis of Ref. [1] is taken *prima facie*, including the radiative (and other) corrections to the finite-size effect. The errors in the radii calculated here are dominated by the experimental error in L_{measured} . Also shown are the values obtained in Ref. [1] and the previously accepted 2006 CODATA value [2].

Name	$\rho(r)$	$\sqrt{\langle r_p^2 \rangle}$ [fm]
exponential	Ae^{-Br}	0.84174(67)
Yukawa	Ae^{-Br}/r	0.84194(67)
Gaussian	Ae^{-Br^2}	0.84155(67)
Ref. [1]		0.84184(67)
CODATA [2]		0.8768(69)

and the remaining coefficients are taken from Table II. Of the three solutions to Eq. (22), only one is physically meaningful. The physically meaningful value of the proton rms charge-radius calculated for each of the choices of charge-distribution are given in Table III and compared in Fig. 4.

We do not calculate a prediction for the proton rms charge radius based on the G_E fitted charge distribution as the above analysis requires knowledge of the polynomial dependence on this quantity, which is absent from this aspect of our investigation. Nonetheless, the similarity between predictions of the finite-size effect at $r_p = 0.878$ fm as given in Eqs. (17–20) suggest that no significant changes would be found.

V. CONCLUSIONS

The dependence of the proton rms charge-radius extracted from an analysis of the measured transition in muonic hydrogen on the choice of proton charge-distribution (and thus form-factor) investigated here is shown to be of negligible importance, despite

the wide range of higher-order moments (given that $\langle r^4 \rangle = 5\langle r^2 \rangle^2/2$ for exponential; $5\langle r^2 \rangle^2/3$ for Gaussian; and $10\langle r^2 \rangle^2/3$ for Yukawa charge-distributions) and investigation of a realistic charge-distribution based on experimental data (of the electric Sachs form factor).

The analysis of Ref. [1] suggests a discrepancy with the 2006 CODATA rms charge-radius of 3.99%. Using the charge-distributions detailed herein, we have calculated a discrepancy with the 2006 CODATA value of 4.02% for Gaussian; 4.00% for exponential; and 3.98% for Yukawa charge-distributions, indicating no significant variation based on this choice alone.

For the purposes of comparison, it is unclear via the references of Ref. [1] which charge-distribution has been used to obtain the value found there. We do conclude however that no choice of charge-distribution is likely to alter the prediction for the proton rms charge-radius in a statistically significant manner, given the wide range of shapes investigated here, and the here confirmed insensitivity of the muonic hydrogen Lamb shift to the shape of the proton charge distribution.

Turning our attention to the recent estimates of Ref. [6] in which the charge-distribution (via the form-factor) dependence of the results of Ref. [1] are challenged—we propose that the results found herein quantify this dependence sufficiently and rule out the shape of the proton form-factor as a source of the proton radius discrepancy.

Acknowledgments

This research was supported in part by the United States Department of Energy (under which Jefferson Science Associates, LLC, operates Jefferson Lab) via contract DE-AC05-06OR23177 (JDC, in part); grant FG02-97ER41014 (GAM); and grant DE-FG02-04ER41318 (JR), and by the Australian Research Council, FL0992247, and the University of Adelaide (JDC, AWT). GAM and JR gratefully acknowledge the support and hospitality of the University of Adelaide while the project was undertaken.

-
- [1] R. Pohl, A. Antognini, F. Nez, F. D. Amaro, F. Biraben, et al., Nature (and Supplementary Material) **466**, 213 (2010).
 - [2] P. J. Mohr, B. N. Taylor, and D. B. Newell, Rev. Mod. Phys. **80**, 633 (2008), 0801.0028.
 - [3] E. Borie, Phys. Rev. A **71**, 032508 (2005), physics/0410051.
 - [4] A. Martynenko, Phys.Atom.Nucl. **71**, 125 (2008), hep-ph/0610226.
 - [5] A. Martynenko, Phys.Rev. **A71**, 022506 (2005), hep-ph/0409107.
 - [6] A. De Rujula, Phys. Lett. **B697**, 26 (2011), 1010.3421.
 - [7] J. D. Carroll, A. W. Thomas, J. Rafelski, and G. A. Miller, Phys. Rev. **A84** (2011), 1104.2971.
 - [8] U. D. Jentschura, Eur. Phys. J. **D61**, 7 (2011), 1012.4029.
 - [9] M. Bawin and S. A. Coon, Nucl. Phys. **A689**, 475 (2001), nucl-th/0101005.
 - [10] W. A. Barker and F. N. Glover, Phys. Rev. **99**, 317 (1955).
 - [11] S. Venkat, J. Arrington, G. A. Miller, and X. Zhan, Phys. Rev. **C83**, 015203 (2011), 1010.3629.
 - [12] J. J. Kelly, Phys. Rev. **C70**, 068202 (2004).
 - [13] K. Pachucki, Phys. Rev. **A60**, 3593 (1999).
 - [14] J. L. Friar, Ann. Phys. **122**, 151 (1979).
 - [15] G. A. Miller, A. W. Thomas, J. D. Carroll, and J. Rafelski, Phys. Rev. **A** (2011), 1101.4073.

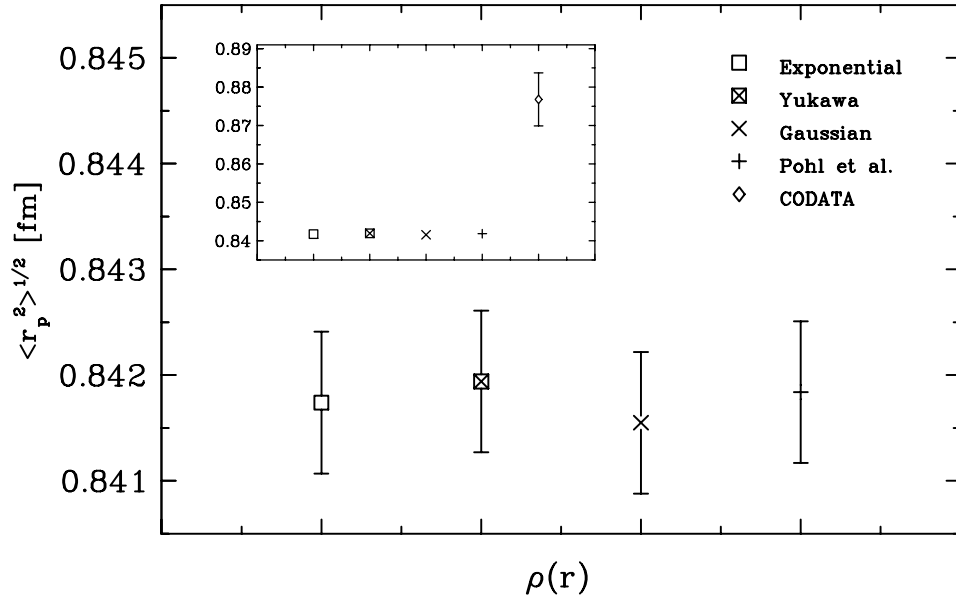


FIG. 4: Comparison of calculated proton rms charge-radii (with errors) for various charge-distributions. Also shown are the values of Pohl et al. from Ref. [1] and (inset) the 2006 CODATA value, Ref. [2]. Error bars are shown for all data here, but in many cases they are not visible. It should be stressed that the analysis of this data remains reliant on the as-yet unknown contribution of off-shell effects [15].